Cooperative Visual Pursuit Control with Learning of Position Dependent Target Motion via Gaussian Process

Junya Yamauchi, Marco Omainska, Thomas Beckers, Takeshi Hatanaka, Sandra Hirche and Masayuki Fujita

***Abstract*— This paper considers a pursuit control based on cooperative target motion estimation by robotic networks equipped with visual sensors. First, we propose a cooperative pursuit control law with a vision-based observer using visual sensor networks, called *networked visual motion observer*. Then, we learn position dependent target motion by a Gaussian process and integrate it within the proposed control law. Second, we show that all rigid bodies converge to desired relative poses when at least one robot can obtain visual information of the target. Furthermore, we prove that the total estimation and control error is ultimately bounded with high probability when integrating a GP model. Finally, we demonstrate the effectiveness of the proposed control law through simulations.**

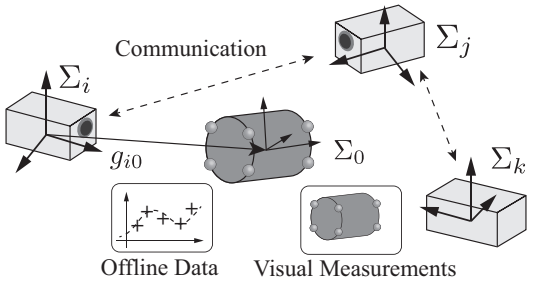

Fig. 1: Cooperative visual pursuit with motion learning.

I. INTRODUCTION

Due to the nature of visual sensors providing rich environmental information, research on autonomy of robots using visual sensors has advanced in the fields of systems and control [1], [2] and machine learning [3]. In this paper, we consider a situation where mobile robots equipped with visual sensors pursue an object. Motivating applications include the prevention of bird strikes [4] and investigation of animal ecology [5]. Since the target motion is unknown, the risk of losing sight must be considered. To this end, this paper considers cooperative pursuit by a group of robots and learns the unknown target motion from data (Fig. 1).

Although vision-based robot control has been traditionally investigated for robot manipulators, control objects have been shifted to mobile robots, including aerial drones [6], [7]. The 3D motion of a mobile robot is typically modeled by so-called rigid body motion, which is a nonlinear system evolving on a matrix manifold. In [2], [8], [9], nonlinear observers are proposed to estimate rigid body motion. In particular, the authors in [2] focus on passivity of rigid body motion, and this paper also focuses on this passivity based method. The observer proposed in [2] is called *visual motion observer* and is used for tracking control. Furthermore, it is extended in [10] to estimate rigid body motion cooperatively by visual sensor networks, which is called *networked visual motion observer*. However, a cooperative control based on this observer has not been considered.

On the other hand, many research results have reported on the use of machine learning techniques for learning unknown dynamics. In particular, Gaussian process (GP) regression based on Bayesian inference is a powerful modeling tool that can quantify the uncertainty of the learned model [11]. In [12]–[15], a GP model is utilized to learn the unknown dynamics and to analyze control performance and stability. The author's recent publication [16] extends the result in [2] with the technique from [14] by integrating the learned GP target motion model into the visual pursuit control scheme, which guarantees stability with high probability.

In this paper, we extend the results of previous works [10], [16] by proposing a control law to pursue a target by a group of robots based on motion estimation and learned target velocities by GP regression. Similar to [16], this paper considers a situation where a target motion is limited by complex environments such as urban and forest sites, and the motion is dependent on its position. The contributions are summarized as: (i) an observer based visual cooperative controller is proposed, (ii) the controller is extended by integrating a GP target motion model, (iii) ultimate boundedness of estimation and control error is shown. The controller of (i) is obtained based on passivity of rigid body motion and the networked visual motion observer proposed in [10]. Then, we extend it to a controller with a GP model in (ii) according to the approach in [16], which is a case of one pursuer. Furthermore, ultimate boundedness in (iii) is also derived based on properties of the graph Laplacian matrix.

This paper is organized as follows: Section II formulates the problem to be considered. In Section III, we propose a control law with an integrated GP model, and then, we analyze the stability in Section IV. Finally, we demonstrate the proposed control scheme by simulations in Section V, and summarizes the results in Section VI.

This work was supported by JSPS KAKENHI Grant Number 20K14761, and partially supported by the European Research Council (ERC) Consolidator Grant "Safe data- driven control for human-centric systems (COMAN)" under grant agreement number 864686.

J. Yamauchi, M. Omainska and M. Fujita are with Department of Information Physics and Computing, The University of Tokyo, Tokyo, Japan junya_yamauchi@ipc.i.u-tokyo.ac.jp

T. Beckers is with the Department of Electrical and Systems Engineering, University of Pennsylvania, USA

T. Hatanaka is with the Department of Systems and Control Engineering, Tokyo Institute of Technology, Tokyo, Japan

S. Hirche is with the Department of Electrical and Computer Engineering, Technical University of Munich, Munich, Germany

II. Problem Setting

A. Rigid Body Motion and Networks

In this paper, we consider a target and n robots $\mathcal{V} \coloneqq \{1, \dots, n\}$ moving in 3D space. In the following, both the target and robots are modeled as rigid bodies. The pose of the i-th rigid body from the world coordinate frame Σ_w is denoted as $(p_{wi}, e^{\hat{\xi}_{wi}\theta_{wi}}) \in SE(3)$, and we use the following notation:

$$g_{wi} = \begin{bmatrix} e^{\hat{\xi}_{wi}\theta_{wi}} & p_{wi} \\ 0 & 1 \end{bmatrix}, \quad i \in \{0\} \cup \mathcal{V} \tag{1}$$

where $\xi_{wi} \in \mathbb{R}^3 (\xi_{wi}^T \xi_{wi} = 1)$ is the axis of rotation and $\theta_{wi} \in \mathbb{R}$ is the angle. The pose of the target is denoted as g_{w0}. The operator $\wedge$ computes $\hat{a}b = a \times b$ for any vector $a, b \in \mathbb{R}^3$, and the operator $\vee$ is the inverse operator of $\wedge$. In the following, $\hat{\xi}_{wi}\theta_{wi}$ is denoted as $\hat{\xi}\theta_{wi}$ for simplicity. Then, defining $V_{wi}^b \coloneqq [(v_{wi}^b)^\top \ (\omega_{wi}^b)^\top]^\top \in \mathbb{R}^6$ as the body velocity, we obtain the following rigid body motion:

$$\dot{g}_{wi} = g_{wi}\hat{V}_{wi}^b, \quad \hat{V}_{wi}^b \coloneqq \begin{bmatrix} \hat{\omega}_{wi}^b & v_{wi}^b \\ 0 & 0 \end{bmatrix} \in \mathbb{R}^{4\times 4}. \tag{2}$$

Refer to [2] for details of rigid body motion. We assume that the pose g_{w0} and body velocity V_{w0}^b of the target are unknown. Each robot is assumed to be able to acquire its own g_{wi}, and the body velocity $V_{wi}^b,\ i \in \mathcal{V}$ is the control input to be designed in this paper. For learnability, the target is assumed to move in a field with a limited range.

Assumption 1: The target is moving in a bounded 3D space. In other words, $p_{w0}(t),\ \forall t \geq 0$ belongs to a compact set $\mathcal{X} \subset \mathbb{R}^3$.

This assumption is naturally satisfied due to the terrain where the target moves.

The relative position and orientation of rigid body j with respect to rigid body i is defined as follows

$$g_{ij} = (p_{ij}, e^{\hat{\xi}\theta_{ij}}) \coloneqq g_{wi}^{-1} g_{wj}. \tag{3}$$

Then, the relative rigid body motion is given by

$$\dot{g}_{ij} = -\hat{V}_{wi}^b g_{ij} + g_{ij}\hat{V}_{wj}^b, \quad i, j \in \{0\} \cup \mathcal{V},\ i \neq j. \tag{4}$$

Since there is no means of communication between the target and each robot, g_{i0} cannot be obtained directly.

Each robot can exchange information with its neighbors, and its communication structure is denoted by a graph $\mathcal{G} = (\mathcal{V}, \mathcal{E}),\ \mathcal{E} \subseteq \mathcal{V} \times \mathcal{V}$. Here, $\mathcal{V}$ is the node set, and $\mathcal{E}$ is the edge set. The set of robots adjacent to a robot $i \in \mathcal{V}$ is denoted by $\mathcal{N}_i = \{j \in \mathcal{V} \mid (i, j) \in \mathcal{E}\}$. In this paper, we assume the following graph:

Assumption 2: The graph $\mathcal{G}$ is fixed and undirected.

Moreover, we denote the graph Laplacian matrix associated with the graph $\mathcal{G}$ as L. For details, refer to [17].

B. Online Data: Visual Measurements

In this section, we specify the information obtained by each robot using its visual sensor. First, we assume that there are m feature points on the target extracted by real time processing such as the method in [18], and the position of each feature point in Σ_0 is $p_0^i \in \mathbb{R}^3,\ i \in \{1, \dots, m\}$. The position $p_i^j \coloneqq [x_i^j\ y_i^j\ z_i^j]^\top \in \mathbb{R}^3$ of the j-th feature point viewed from the i-th robot coordinate frame Σ_i is obtained as $[p_i^j\ 1]^\top = g_{i0}[p_0^j\ 1]^\top$. Then, we consider a monocular camera as the visual sensor and use the perspective projection model shown in Fig. 2. The position of each feature point $f_i^j \in \mathbb{R}^2$ on the image plane is given by

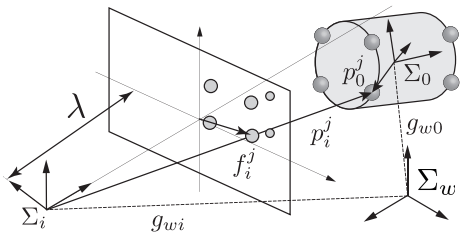

Fig. 2: Perspective projection.

$$f_i^j = (\lambda / z_i^j)\begin{bmatrix} x_i^j & y_i^j \end{bmatrix}^\top, \tag{5}$$

where $\lambda \in \mathbb{R}$ is the focal length of the camera [6]. The stacked vector of f_i^j is denoted as $f_i \coloneqq [(f_i^1)^\top \dots (f_i^m)^\top]^\top$ and called *visual measurement* for i-th robot.

In this paper, we assume a situation where some robots cannot capture m feature points. The set of robots that can acquire m feature points is defined as $\mathcal{V}_v$ called *visibility set*, and the set of the other robots is denoted as $\bar{\mathcal{V}}_v$. Here, we introduce the following:

$$v_i \coloneqq \begin{cases} 1 & \text{if } i \in \mathcal{V}_v \\ 0 & \text{otherwise} \end{cases}, \tag{6}$$

where we assume $v_i,\ i \in \mathcal{V}$ are fixed, i.e., the visibility set $\mathcal{V}_v$ is fixed. Furthermore, using positive real numbers $d_i,\ i \in \mathcal{V}$ we define the followings:

$$D_v = \mathrm{diag}(d_1 v_1, \dots, d_n v_n) \in \mathbb{R}^{n\times n} \tag{7}$$

$$H \coloneqq L + D_v. \tag{8}$$

Then, the matrix H has the following property.

Proposition 1: Suppose that the graph $\mathcal{G}$ satisfies Assumption 2 and $\mathcal{V}_v \neq \emptyset$. Then, H is positive definite.

C. Offline Data

Next, we specify the data obtained by offline information processing. These data are assumed to be difficult to obtain in real time due to large computational cost, noisy measurements, etc. We assume here that we can obtain the target position p_{w0} and the corresponding body velocity offline as

$$y = V_{w0}^b(p_{w0}) + \epsilon, \tag{9}$$

where $\epsilon \coloneqq [\epsilon_1 \cdots \epsilon_6]^\top \in \mathbb{R}^6$ and $\epsilon_i \sim \mathcal{N}(0, \sigma_{ni}^2)$. In addition, ϵ_i is bounded by σ_{ni}, namely $|\epsilon_i| \leq \sigma_{ni}$. We assume that the dataset consisting of M training inputs $\{p_{w0}^{\{i\}}\}_{i=1}^M$ and outputs $\{y^{\{i\}}\}_{i=1}^M$ is available and denoted as

$$X \coloneqq \begin{bmatrix} p_{w0}^{\{1\}} & \cdots & p_{w0}^{\{M\}} \end{bmatrix}^\top,\ Y \coloneqq \begin{bmatrix} y^{\{1\}} & \cdots & y^{\{M\}} \end{bmatrix}^\top, \tag{10}$$
$$\mathcal{D} \coloneqq \{X, Y\}.$$

The dataset is utilized for prediction of $V^b_{w0}(p^*_{w0})$ at the new position p^*_{w0}. We also assume that the function $V^b_{w0}(p^*_{w0})$ is an element of a Reproducing Kernel Hilbert Space. This is a mild assumption since it only excludes irregularity such as discontinuity from a class of considered functions.

D. Control Objective

In this paper, we consider to drive g_{i0} to constant desired poses $g_{di} = (p_{di}, e^{\hat{\xi}\theta_{di}}) \in SE(3),\ i \in \mathcal{V}$. To describe this objective, we define the control error as

$$\tilde{e}_{ci} \coloneqq vec(g_{di}^{-1} g_{i0}), \quad i \in \mathcal{V} \tag{11}$$

where $vec(\cdot)$ is the operator for $g \in SE(3)$ to obtain

$$vec(g) \coloneqq \left[p^\top (\mathrm{sk}(e^{\hat{\xi}\theta})^\vee)^\top\right]^\top,\ \mathrm{sk}(e^{\hat{\xi}\theta}) \coloneqq \frac{1}{2}(e^{\hat{\xi}\theta} - e^{-\hat{\xi}\theta}).$$

When $\tilde{e}_{ci} \to 0,\ \forall i \in \mathcal{V}$, the objective is accomplished. However, the accomplishment is difficult because predictions by machine learning techniques is not perfect. Based on the above discussion, we formulate the problem to be solved.

Problem 1: Suppose that all robots are connected by the graph $\mathcal{G}$. Further assume that $g_{wi},\ i \in \mathcal{V}$, the visual measurements (5) and the dataset (10) are available. Then, design a visual pursuit control law that achieves $\lim_{t\to\infty} \|\tilde{e}_{ci}\| \leq B,\ \forall i \in \mathcal{V}$ with a given nonnegative constant B.

Since the robots can only get visual measurements of the target, g_{i0} is not measurable directly. Therefore, we introduce the visual motion observer to estimate g_{i0} and reformulate Problem 1 with motion estimation in the next section.

III. Cooperative Visual Pursuit Control

In this section, we first introduce the visual motion observer and reformulate Problem 1. Then, we propose a control law as a solution to the problem.

A. Visual Motion Observer and Error System

Estimation of the relative pose g_{i0}, which is not obtained directly from visual sensors, is denoted as $\bar{g}_i = (\bar{p}_i, e^{\hat{\bar{\xi}}\bar{\theta}_i}) \in SE(3)$. Based on [2], we introduce the following model to estimate the relative rigid body motion:

$$\dot{\bar{g}}_i = -\hat{V}^b_{wi}\bar{g}_i - \bar{g}_i\hat{u}_{ei}, \quad i \in \mathcal{V}, \tag{12}$$

where $u_{ei} \in \mathbb{R}^6$ is the observer input to be designed. Then, we define estimation error as

$$g_{ei} = (p_{ei}, e^{\hat{\xi}\theta_{ei}}) \coloneqq \bar{g}_i^{-1} g_{i0}, \quad e_{ei} \coloneqq vec(g_{ei}). \tag{13}$$

Here, e_{ei} is the error between the true relative pose g_{i0} and the estimate $\bar{g}_i$, so it cannot be calculated directly. However, if $m \geq 4$, it can be reconstructed as $e_{ei} = J_i^\dagger(f_i - \bar{f}_i)$ using the pseudo-inverse of the image Jacobian J_i [2]. $\bar{f}_i$ is an estimate of the visual measurement obtained from the estimate $\bar{g}_i$ and (5). Then, the time evolution of g_{ei} obeys

$$\dot{g}_{ei} = \hat{u}_{ei}g_{ei} + g_{ei}\hat{V}^b_{w0}. \tag{14}$$

Next, we redefine the control error with $\bar{g}_i$ as

$$g_{ci} = (p_{ci},\ e^{\hat{\xi}\theta_{ci}}) \coloneqq g_{di}^{-1}\bar{g}_i, \quad e_{ci} \coloneqq vec(g_{ci}). \tag{15}$$

The time evolution of the control error obeys

$$\dot{g}_{ci} = \hat{u}_{ci}g_{ci} - g_{ci}\hat{u}_{ei}, \tag{16}$$

where $u_{ci} \coloneqq -\mathrm{Ad}_{(g_{di}^{-1})}V^b_{wi}$. The matrix $\mathrm{Ad}_{(g)} \in \mathbb{R}^{6\times 6}$ is the adjoint transformation [2] and is defined as

$$\mathrm{Ad}_{(g)} \coloneqq \begin{bmatrix} e^{\hat{\xi}\theta} & \hat{p}e^{\hat{\xi}\theta} \\ 0 & e^{\hat{\xi}\theta} \end{bmatrix}. \tag{17}$$

For simplicity of notation, the adjoint transformation for $(0, e^{\hat{\xi}\theta})$ is denoted by $\mathrm{Ad}_{(e^{\hat{\xi}\theta})}$. In this paper, u_{ci} is to be designed and the body velocity is applied to each robot as $V^b_{wi} = -\mathrm{Ad}_{(g_{di})}u_{ci},\ i \in \mathcal{V}$. Hereafter, the system consists of (14) and (16) is referred to as *error system* for i-th robot.

B. Control Objective with Motion Estimation

We define the following stacked forms of the estimation and control errors as

$$e_c \coloneqq [e_{c1}^\top \dots e_{cn}^\top]^\top,\ e_e \coloneqq [e_{e1}^\top \dots e_{en}^\top]^\top, \tag{18}$$

$$e_i \coloneqq [e_{ci}^\top\ e_{ei}^\top]^\top \in \mathbb{R}^{12}\ e \coloneqq [e_c^\top\ e_e^\top]^\top \in \mathbb{R}^{12n}. \tag{19}$$

Then, Problem 1 is modified by considering motion estimation of the target as follow:

Problem 2: Suppose that all robots are connected by the graph $\mathcal{G}$. Further assume that $g_{wi},\ i \in \mathcal{V}$, the visual measurements (5) and the dataset (10) are available. Then, design a visual pursuit control law that achieves

$$\lim_{t\to\infty} \|e(t)\| \leq B, \quad B \geq 0. \tag{20}$$

C. Control Law

In this section, we propose an observer and control input $u_i \coloneqq [u_{ci}^\top\ u_{ei}^\top]^\top \in \mathbb{R}^{12}$ as a solution for Problem 2 based on passivity of the error system.

To see passivity of the error system, we define the following energy function:

$$S_i \coloneqq \frac{1}{2}\|p_{ei}\|^2 + \frac{1}{2}\phi(e^{\hat{\xi}\theta_{ei}}) + \frac{1}{2}\|p_{ci}\|^2 + \frac{1}{2}\phi(e^{\hat{\xi}\theta_{ci}}), \tag{21}$$

for $i \in \mathcal{V}$, where ϕ is defined as $\phi(e^{\hat{\xi}\theta}) \coloneqq (1/2)\|I_3 - e^{\hat{\xi}\theta}\|_F^2 = \mathrm{tr}(I_3 - e^{\hat{\xi}\theta})$. In addition, we define

$$N_i \coloneqq \begin{bmatrix} I_6 & 0 \\ -\mathrm{Ad}_{(e^{-\hat{\xi}\theta_{ci}})} & I_6 \end{bmatrix} \in \mathbb{R}^{12\times 12}. \tag{22}$$

Then we obtain the following corollary [2, Corollary 7.1].

Lemma 1: The time derivative of the energy function S_i along the trajectory of the error system is obtained as

$$\dot{S}_i = e_i^\top N_i^\top u_i + e_i^\top \begin{bmatrix} 0 \\ \mathrm{Ad}_{(e^{\hat{\xi}\theta_{ei}})} \end{bmatrix} V^b_{w0}, \quad i \in \mathcal{V}, \tag{23}$$

where $u_i = [u_{ci}^\top\ u_{ei}^\top]^\top \in \mathbb{R}^{12}$.

When the target is static ($V^b_{w0} \equiv 0$), the error system for i-th robot is passive from u_i to $N_i e_i$ with respect to S_i. Thus, if all the robots belong to $\mathcal{V}_v$, the negative feedback of $N_i e_i$ makes the error system stable. However, if there is a robot that does not belong to $\mathcal{V}_v$, this robot cannot apply this negative feedback because the robot cannot obtain e_{ei} from (5). In [10], the networked visual motion

observer is proposed which estimates the target motion while synchronizing $\bar{g}_{w,i} = (\bar{p}_{w,i}, e^{\hat{\xi}\bar{\theta}_{w,i}}) \coloneqq g_{wi}\bar{g}_i$ between robots. Here, $\bar{g}_{w,i}$ is the estimate of g_{w0} by i-th robot.

Based on passivity and the result in [10], we propose the control law as follow:

$$u_i = -K_i N_i e_i - k_s R_i \sum_{j\in\mathcal{N}_i} vec(\bar{g}_{w,i}^{-1}\bar{g}_{w,j}), \quad k_s > 0 \quad (24)$$

where $R_i \coloneqq [I_6 \ \mathrm{Ad}_{(e^{\hat{\xi}\theta_{ci}})}]^\top$ and the gain K_i with positive constants k_{cij}, k_{eij} is designed as

$$K_{ci} = \mathrm{diag}(k_{ci1}, \cdots, k_{ci6}),\ K_{ei} = \mathrm{diag}(k_{ei1}I_3, k_{ei2}I_3),$$
$$K_i = \mathrm{diag}(K_{ci},\ v_i K_{ei}) \in \mathbb{R}^{12\times 12}. \quad (25)$$

When only $n = 1$ robot is considered, the control law coincides with [2]. When $e_{ci} = 0$, (24) coincides with the observer input in [10]. Additionally, we obtain $\dot{\bar{g}}_{w,i} = -\bar{g}_{w,i}\hat{u}_{ei}$, and substituting u_{ei} in (24) with $K_{ei} = 0$ yields $\dot{\bar{g}}_{w,i} = k_s\bar{g}_{w,i}\sum_{j\in\mathcal{N}_i} vec(\bar{g}_{w,i}^{-1}\bar{g}_{w,j})^\wedge$. This is consistent with synchronization law on $SE(3)$ in [19]. In other words, u_{ei} with $K_{ei} = 0$ is the observer input to synchronize the estimates $\bar{g}_{w,i}$ in the group of rigid bodies.

D. Learning of Target Body Velocities by Gaussian Process

Since the body velocity is a function of the target position $p_{w0} \in \mathcal{X}$ and an element of a Reproducing Kernel Hilbert Space (RKHS), it is possible to learn the probabilistic model by Gaussian process regression from the dataset $\mathcal{D}$ in (10). To establish a model of $V_{w0}^b(p_{w0})$, we use the squared exponential (SE) kernel given by

$$k_i(p_{w0}, p'_{w0}) = \sigma_{fi}^2 \exp\left(-\sum_{j=1}^{3}\frac{([p_{w0}]_j - [p'_{w0}]_j)^2}{2l_{ij}^2}\right), \quad (26)$$

where $[\cdot]_i$ denotes i-th element of vectors. The signal variance $\sigma_{fi}^2 > 0$ and the lengthscales $l_{ij} > 0$ are called *hyperparameters* and typically trained by evidence maximization [11]. Here, we denote ij-th element of a matrix as $[\cdot]_{ij}$. Then, we define the kernel matrix as $[\mathcal{K}_i]_{jl} \coloneqq k_i(p_{w0}^{\{j\}}, p_{w0}^{\{l\}})$ and kernel vector as $[k_{i*}]_j \coloneqq k_i(p_{w0}^*, p_{w0}^{\{j\}})$ with a new input p_{w0}^*. Let $Y_i \in \mathbb{R}^M$ be the i-th column of Y. Then, the mean and variance of y^* for a new input p_{w0}^* is obtained as

$$\mu_i(y^* \mid \mathcal{D}, p_{w0}^*) = k_{i*}^\top(\mathcal{K}_i + \sigma_{ni}^2 I_M)^{-1}Y_i,$$
$$\mathrm{var}_i(y^* \mid \mathcal{D}, p_{w0}^*) = k_i(p_{w0}^*, p_{w0}^*) - k_{i*}^\top(\mathcal{K}_i + \sigma_{ni}^2 I_M)^{-1}k_{i*}.$$

Furthermore, we define the following stacked vector $\mu_i(y^* \mid \mathcal{D}, p_{w0}^*)$ and diagonal matrix of $\mathrm{var}_i(y^* \mid \mathcal{D}, p_{w0}^*)$:

$$\mu(p_{w0}^*) = [\mu_1 \dots \mu_6]^\top \in \mathbb{R}^6, \quad (27a)$$
$$\Sigma(p_{w0}^*) = \mathrm{diag}(\mathrm{var}_1, \dots, \mathrm{var}_6) \in \mathbb{R}^{6\times 6}. \quad (27b)$$

Then, the result of [20, Theorem 6] gives us an upper bound related to model fidelity with the bounded norm $\|[V_{w0}^b]_i\|_{k_i},\ i \in \{1, \dots, 6\}$ associated with k_i.

Lemma 2: Consider a Gaussian process trained from the dataset $\mathcal{D}$ in (10). Then, the model error is bounded by

$$P\{\forall p_{w0} \in \mathcal{X}, \|\mu(p_{w0}) - V_{w0}^b(p_{w0})\| \le \|\beta^\top \Sigma^{\frac{1}{2}}(p_{w0})\|\} \ge \delta \quad (28)$$

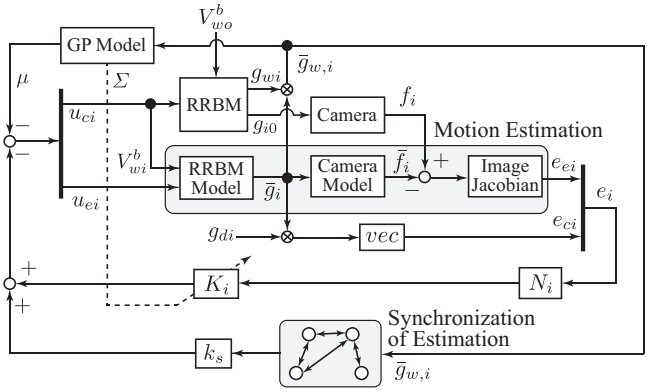

Fig. 3: Block diagram of cooperative visual pursuit control. "RRBM" is an acronym of Relative Rigid Body Motion.

with probability $\delta \in (0, 1)$, and $\beta \in \mathbb{R}^6$ is defined as $[\beta]_i \coloneqq \sqrt{2\|[V_{w0}^b]_i\|_{k_i}^2 + 300\zeta_i \ln^3\left(\frac{M+1}{1-\delta^{1/6}}\right)}$ with the maximum information gain $\zeta_i \in \mathbb{R}$.

Since the SE kernel is an universal kernel, it can approximate any continuous function arbitrarily precisely on a compact set. Thus, even if $[V_{w0}^b]_i$ is not an element of the RKHS associated with k_i and $\|[V_{w0}^b]_i\|_{k_i}$ is not bounded, it is still bounded for a function arbitrarily close to $[V_{w0}^b]_i$ [14].

E. Control Law with Target Motion Model by GP

Next, we consider the case of the moving target with (30). In [16], a visual pursuit control law using GP is proposed for single robot case. According to the result, we consider integrating the control law of [16] and the cooperative visual pursuit control law (24). We also consider adjusting K_i by the variance of GP in the same way as [16] for reflecting the uncertainty of prediction. Design $k_{cij} \circ \Sigma$ and $k_{eij} \circ \Sigma$ to be continuous on $\bar{p}_{w,i} \in \mathbb{R}^3$ and satisfy

$$\underline{k}_c \le k_{cij}(\Sigma(\bar{p}_{w,i})) \le \bar{k}_c,\ \underline{k}_e \le k_{eij}(\Sigma(\bar{p}_{w,i})) \le \bar{k}_e, \quad (29)$$

where $\underline{k}_c$, $\bar{k}_c$, $\underline{k}_e$ and $\bar{k}_e$ are positive constants. Note that the argument of Σ is replaced by $\bar{p}_{w,i}$ since p_{w0} is not available online. Now, we propose the following control law:

$$\begin{aligned} u_i = &- K_i(\Sigma(\bar{p}_{w,i}))N_i e_i - A_i\mu(\bar{p}_{w,i}) \\ &- k_s R_i \sum_{j\in\mathcal{N}_i} vec(\bar{g}_{w,i}^{-1}\bar{g}_{w,j}), \end{aligned} \quad (30)$$

where the matrix $A_i \in \mathbb{R}^{12\times 6}$ is defined as $A_i \coloneqq \left[\mathrm{Ad}_{(e^{-\hat{\xi}\theta_{ei}})}\mathrm{Ad}_{(e^{-\hat{\xi}\theta_{ci}})}\ \ \mathrm{Ad}_{(e^{-\hat{\xi}\theta_{ei}})}\right]^\top$[1]. The first and third terms of (30) are the same as in (24), and the first and second terms are the same as in [16]. The block diagram of the addressed system with (30) is depicted in Fig. 3.

IV. Stability Analysis

In this section, we first analyze the stability with the control law (24) when the target is static and verify that

[1]The matrix $e^{\hat{\xi}\theta_{ei}}$ used in A_i can be obtained as $e^{\hat{\xi}\theta_{ei}} = \exp\Big((\sin^{-1}(\|\mathrm{sk}(e^{\hat{\xi}\theta_{ei}})^\vee\|))/(\|\mathrm{sk}(e^{\hat{\xi}\theta_{ei}})^\vee\|)\mathrm{sk}(e^{\hat{\xi}\theta_{ei}})\Big)$.

Problem 2 is solved. Next, we analyze the case where the control law (30) is applied to a moving target.

A. Case of Static Target

Applying the control law (24) to the error system, we obtain the following theorem.

Theorem 1: Consider the error system consisting of (14), (16) and (24), and the graph $\mathcal{G}$ satisfying Assumption 2 with $\mathcal{V}_v = \mathcal{V}$. Suppose that the target is static and $e^{\hat{\xi}\theta_{ei}} > 0,\ \forall i \in \mathcal{V},\ \forall t \geq 0$[2]. Then, (20) is achieved with $B = 0$.

Proof: First, we define the following based on (21).

$$S \coloneqq \sum_{i\in\mathcal{V}} S_i \tag{31}$$

Then, $\dot{S}$ is obtained from the input in Lemma 1 and (24) as

$$\begin{aligned}\dot{S} = &-\sum_{i\in\mathcal{V}} e_i^\top N_i^\top K_i N_i e_i \\ &- k_s \sum_{i\in\mathcal{V}}\sum_{j\in\mathcal{N}_i} e_i^\top N_i^\top R_i vec(\bar{g}_{w,i}^{-1}\bar{g}_{w,j}).\end{aligned} \tag{32}$$

Since the matrix $N_i^\top K_i N_i$ is positive definite and $\mathcal{V}_v = \mathcal{V}$, $\dot{S}$ is negative definite if the second term of (32) is negative.

From the definitions of N_i and R_i, $e_i^\top N_i^\top R_i vec(\bar{g}_{w,i}^{-1}\bar{g}_{w,j}) = e_{ei}^\top vec(\bar{g}_{w,i}^{-1}\bar{g}_{w,j})$. It is further decomposed into $p_{ei}^\top e^{-\hat{\xi}\bar{\theta}_{w,i}}(\bar{p}_{w,j} - \bar{p}_{w,i})$ and $(\mathrm{sk}(e^{\hat{\xi}\theta_{ei}})^\vee)^\top \mathrm{sk}(e^{-\hat{\xi}\bar{\theta}_{w,i}}e^{\hat{\xi}\bar{\theta}_{w,j}})^\vee$. From the fact that $p_{ei} = e^{-\hat{\xi}\bar{\theta}_{w,i}}(p_{w0} - \bar{p}_{w,i})$ and Assumption 2, we have

$$\begin{aligned}&\sum_{i\in\mathcal{V}}\sum_{j\in\mathcal{N}_i}(p_{w0} - \bar{p}_{w,i})^\top(\bar{p}_{w,j} - \bar{p}_{w,i}) \\ &\qquad = \sum_{i\in\mathcal{V}}\sum_{j\in\mathcal{N}_i}\|\bar{p}_{w,i} - \bar{p}_{w,j}\|^2 \geq 0.\end{aligned} \tag{33}$$

Next, from Assumption 2, we have,

$$\begin{aligned}&\sum_{i\in\mathcal{V}}\sum_{j\in\mathcal{N}_i}(\mathrm{sk}(e^{-\hat{\xi}\bar{\theta}_{w,i}}e^{\hat{\xi}\theta_{w0}})^\vee)^\top \mathrm{sk}(e^{-\hat{\xi}\bar{\theta}_{w,i}}e^{\hat{\xi}\bar{\theta}_{w,j}})^\vee \\ &\geq \frac{1}{2}\sum_{i\in\mathcal{V}}\sum_{j\in\mathcal{N}_i}\rho_i\phi(e^{-\hat{\xi}\bar{\theta}_{w,i}}e^{\hat{\xi}\bar{\theta}_{w,j}}) \geq 0,\end{aligned} \tag{34}$$

since $e^{\hat{\xi}\theta_{ei}} = e^{-\hat{\xi}\bar{\theta}_{w,i}}e^{\hat{\xi}\theta_{w0}}$, where ρ_i denotes the smallest eigenvalue of $(1/2)(e^{\hat{\xi}\theta_{ei}} + e^{-\hat{\xi}\theta_{ei}})$ and it is positive when $e^{\hat{\xi}\theta_{ei}}$ is positive definite [2, Lemma E.2 and Proposition C.2]. Therefore, from (33) and (34), the second term of (32) becomes negative. Thus, $\dot{S} \leq -\sum_{i\in\mathcal{V}} e_i^T N_i^T K_i N_i e_i < 0$. and hence, (20) is held with $B = 0$. ■

Next, we show the result with $\mathcal{V}_v \neq \mathcal{V}$.

Theorem 2: Consider the error system consisting of (14), (16) and (24), and the graph $\mathcal{G}$ satisfying Assumption 2 with $\mathcal{V}_v \neq \emptyset$. Then, if the target is static and $e^{\hat{\xi}\theta_{ei}} > 0,\ \forall i \in \mathcal{V},\ \forall t \geq 0$, (20) is achieved with $B = 0$.

[2]The assumption implies that all rotation estimation error should stay inside the half-sphere centered at I_3, which is in general satisfied in the considered scenario in this paper.

Proof: First, we consider (32)–(34) and define

$$\begin{aligned}U &\coloneqq \sum_{i\in\mathcal{V}} e_i^T N_i^T K_i N_i e_i, \\ W &\coloneqq \frac{k_s}{2}\sum_{i\in\mathcal{V}}\sum_{j\in\mathcal{N}_i}(\|\bar{p}_{w,i} - \bar{p}_{w,j}\|^2 + \rho_i\phi(e^{-\hat{\xi}\bar{\theta}_{w,i}}e^{\hat{\xi}\bar{\theta}_{w,j}})).\end{aligned}$$

Then, we can simply denote (32) as $\dot{S} \leq -U - W$. Furthermore, we define the following:

$$P_e \coloneqq [\|p_{ei}\| \cdots \|p_{en}\|]^\top \in \mathbb{R}^n, \tag{35}$$

$$\Phi_e \coloneqq \left[\phi^{\frac{1}{2}}(e^{\hat{\xi}\theta_{e1}}) \cdots \phi^{\frac{1}{2}}(e^{\hat{\xi}\theta_{en}})\right]^\top \in \mathbb{R}^n. \tag{36}$$

Here, $N_i^\top K_i N_i$ is a positive definite matrix for $i \in \mathcal{V}_v$, and $N_i^\top K_i N_i = \mathrm{diag}(K_{ci}, 0)$ for $i \in \bar{\mathcal{V}}_v$. Let λ_{Ki} be the smallest eigenvalue of $N_i^\top K_i N_i$ for $i \in \mathcal{V}_v$ and the smallest eigenvalue of K_{ci} for $i \in \bar{\mathcal{V}}_v$, then $\lambda_{Ki} > 0,\ \forall i \in \mathcal{V}$. Also, since $\phi(e^{\hat{\xi}\theta}) \leq 2\|\mathrm{sk}(e^{\hat{\xi}\theta})^\vee\|^2$ holds when $e^{\hat{\xi}\theta} > 0$ [2, Proposition 5.3], we have

$$\begin{aligned}U &\geq \sum_{i\in\mathcal{V}_v}\lambda_{Ki}\|e_{ei}\|^2 + \sum_{i\in\mathcal{V}}\lambda_{Ki}\|e_{ci}\|^2 \\ &\geq \sum_{i\in\mathcal{V}_v}\lambda_{Ki}\|p_{ei}\|^2 + \frac{1}{2}\sum_{i\in\mathcal{V}_v}\lambda_{Ki}\phi(e^{\hat{\xi}\theta_{ei}}) + e_c^\top\Lambda e_c \\ &\geq P_e^\top D_v P_e + \Phi_e^\top D_v \Phi_e + e_c^\top\Lambda e_c,\end{aligned} \tag{37}$$

where $\Lambda \coloneqq \mathrm{diag}(\lambda_{K1}, \ldots, \lambda_{Kn}) \otimes I_6$, and we set $d_i = (1/2)\lambda_{Ki}$ in (7).

Next, we consider W. From $\bar{p}_{w,i} = -e^{-\hat{\xi}\bar{\theta}_{w,i}}p_{ei} + p_{w0}$ and the reverse triangle inequality, we have $\|\bar{p}_{w,i} - \bar{p}_{w,j}\| \geq |\|p_{ei}\| - \|p_{ej}\||$. Futhermore, from $e^{\hat{\xi}\bar{\theta}_{w,i}} = e^{\hat{\xi}\theta_{w0}}e^{-\hat{\xi}\theta_{ei}}$, we have $2\phi(e^{-\hat{\xi}\bar{\theta}_{w,i}}e^{\hat{\xi}\theta_{w,j}}) = \|e^{\hat{\xi}\theta_{ei}} - e^{\hat{\xi}\theta_{ej}}\|_F^2$. Here, from the reverse triangle inequality, we obtain $\|(I - e^{\hat{\xi}\theta_{ei}}) - (I - e^{\hat{\xi}\theta_{ej}})\|_F \geq |\|I - e^{\hat{\xi}\theta_{ei}}\|_F - \|I - e^{\hat{\xi}\theta_{ej}}\|_F|$. Then, squaring both sides and multiplying by $1/2$ yields $\phi(e^{-\hat{\xi}\theta_{w,i}}e^{\hat{\xi}\theta_{w,j}}) \geq \left(\phi^{\frac{1}{2}}(e^{\hat{\xi}\theta_{ei}}) - \phi^{\frac{1}{2}}(e^{\hat{\xi}\theta_{ej}})\right)^2$. When $e^{\hat{\xi}\theta_{ei}} > 0$, there exists a ϵ such that $|\theta_{ei}| \leq \pi/2 + \epsilon$ for all $i \in \mathcal{V}$, namely, $\sin\epsilon \leq \rho_i$ [2, Proposition C.2]. Therefore, we have

$$\begin{aligned}W \geq\ &\frac{1}{2}k_s\sin\epsilon\sum_{i\in\mathcal{V}}\sum_{j\in\mathcal{N}_i}\Bigg((\|p_{ei}\| - \|p_{ej}\|)^2 \\ &+ \left(\phi^{\frac{1}{2}}(e^{\hat{\xi}\theta_{ei}}) - \phi^{\frac{1}{2}}(e^{\hat{\xi}\theta_{ej}})\right)^2\Bigg)\end{aligned} \tag{38}$$

$$= P_e^\top L P_e + \Phi_e^\top L \Phi_e \tag{39}$$

where $(1/2)k_s\sin\epsilon$ is the common weight in L. Therefore, (8), (37) and (39), we have $\dot{S} \leq -P_e^\top H P_e - \Phi_e^\top H \Phi_e - e_c^\top\Lambda e_c$. Thus, $\dot{S} < 0$ holds since the matrix H is positive definite from Proposition 1. Hence, it is proved that the equilibrium point $e = 0$ is asymptotically stable. ■

In Theorem 2, by deriving the estimation error e_{ei} from the network term W, the positive definite matrix H appears. This matrix plays an essential role in the next section.

B. Case of Moving Target with GP

We define $\bar{p}_w \coloneqq [\bar{p}_{w,1}^\top \cdots \bar{p}_{w,n}^\top]^\top$, and denote the minimum eigenvalue of H in (8) as λ_H. Note that the elements of H depend on $\bar{p}_w$ since the gains $K_i,\ i \in \mathcal{V}$ in (25) and (29) are adapted by $\Sigma(\bar{p}_{w,i})$. Therefore, λ_H also depends on $\bar{p}_w$. All elements of H are determined in Theorem 2.

Then, we are now ready to show the main theorem.

Theorem 3: Consider the error system (14), (16) and (30) with the trained GP model (27) with dataset $\mathcal{D}$ (10), and the graph $\mathcal{G}$ satisfying Assumption 2 with $\mathcal{V}_v \neq \emptyset$. Suppose that the target motion satisfies Assumptions 1 and $e^{\hat{\xi}\theta_{ci}} > 0,\ e^{\hat{\xi}\theta_{ei}} > 0$ for all $i \in \mathcal{V}$ and $t \geq 0$. Furthermore, suppose that $\lambda_H(\bar{p}_w)$ satisfies the following condition:

$$\kappa(\bar{p}_w) \coloneqq \lambda_H(\bar{p}_w) - \frac{1}{2\gamma^2} - L_\mu > 0, \quad \forall \bar{p}_w \in \mathbb{R}^{3n}, \tag{40}$$

where γ is a positive constant and L_μ is a Lipschitz constant of μ. Define $\underline{\kappa} \coloneqq \min_{\bar{p}_w \in \mathbb{R}^{3n}} \kappa(\bar{p}_w)$, then, there exist a $\rho(\delta) > 0$ and a $T(\delta) \geq 0$ with any probability $\delta \in (0,1)$ such that

$$\mathcal{P}\{\|e(t)\| \leq B, \forall t \geq T\} \geq \delta \tag{41}$$

$$B(\delta) \coloneqq \frac{n\gamma\bar{\Delta}(\delta)}{\sqrt{\eta\underline{\kappa}}}, \quad \eta \in (0,1) \tag{42}$$

for any $e(0)$ satisfying $\|e(0)\| \leq \rho(\delta)$, where $\bar{\Delta}(\delta)$ is the upper bound of the model error $\|\beta(\delta)^\top \Sigma^{\frac{1}{2}}\|$.

Proof: First, we examine the time evolution of S. From the proof of Theorem 2, we obtain the following:

$$\begin{aligned}\dot{S} \leq & -P_e^\top H P_e - \Phi_e^\top H \Phi_e - e_c^\top \Lambda e_c \\ & + \sum_{i\in\mathcal{V}} e_i^\top \begin{bmatrix} 0 \\ \mathrm{Ad}_{(e^{\hat{\xi}\theta_{ei}})} \end{bmatrix} (V_{w0}^b(p_{w0}) - \mu(\bar{p}_{w,i})).\end{aligned} \tag{43}$$

From Cauchy–Schwarz inequality, we have

$$\begin{aligned}\dot{S} \leq & -P_e^\top H P_e - \Phi_e^\top H \Phi_e - e_c^\top \Lambda e_c \\ & + \sum_{i\in\mathcal{V}} \|e_{ei}\| \|V_{w0}^b(p_{w0}) - \mu(\bar{p}_{w,i})\|.\end{aligned} \tag{44}$$

Since μ is continuous, there exists a Lipschitz constant L_μ [11]. Therefore, from $\bar{p}_{w,i} = -e^{-\hat{\xi}\bar{\theta}_{w,i}} p_{ei} + p_{w0}$, we obtain

$$\begin{aligned}&\|V_{w0}^b(p_{w0}) - \mu(\bar{p}_{w,i})\| \\ &\quad \leq \|V_{w0}^b(p_{w0}) - \mu(p_{w0})\| + \|\mu(p_{w0}) - \mu(\bar{p}_{w,i})\| \\ &\quad \leq \|V_{w0}^b(p_{w0}) - \mu(p_{w0})\| + L_\mu \|p_{ei}\|.\end{aligned} \tag{45}$$

Furthermore, from Peter-Paul inequality, we obtain

$$\begin{aligned}&\|e_{ei}\| \|V_{w0}^b(p_{w0}) - \mu(p_{w0})\| \\ &\qquad \leq \frac{1}{2\gamma^2}\|e_e\|^2 + \frac{\gamma^2}{2}\|V_{w0}^b(p_{w0}) - \mu(p_{w0})\|^2\end{aligned} \tag{46}$$

and $\|e_{ei}\|\|p_{ei}\| \leq \|e_{ei}\|^2$. Then, from (44)–(46), we obtain

$$\begin{aligned}\dot{S} \leq & -P_e^\top H P_e - \Phi_e^\top H \Phi_e - e_c^\top \Lambda e_c + (\frac{1}{2\gamma^2} + L_\mu)\|e_e\|^2 \\ & + \frac{n\gamma^2}{2}\|V_{w0}^b(p_{w0}) - \mu(p_{w0})\|^2\end{aligned} \tag{47}$$

$$\leq -\kappa\|e_e\|^2 - e_c^\top \Lambda e_c + \frac{n\gamma^2}{2}\|V_{w0}^b(p_{w0}) - \mu(p_{w0})\|^2, \tag{48}$$

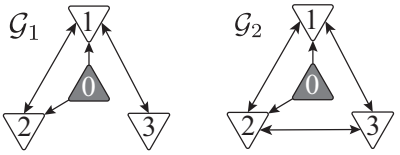

Fig. 4: The graphs $\mathcal{G}_1$ and $\mathcal{G}_2$ with $\mathcal{V}_v = \{1, 2\}$.

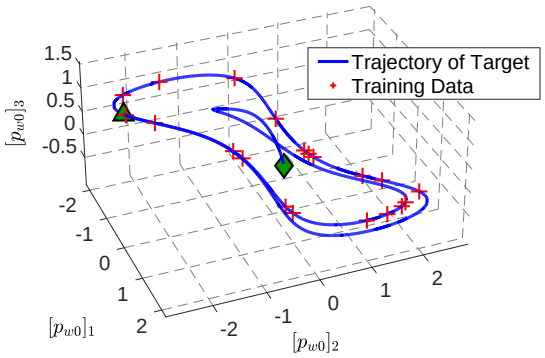

Fig. 5: Trajectory of target generated by (50) and (51). Initial and final position of the target are shown by diamond and triangle in green, respectively.

where we used the fact that $\phi(e^{\hat{\xi}\theta}) \geq \|\mathrm{sk}(e^{\hat{\xi}\theta})^\vee\|^2$ [2, Proposition 5.3]. Here, κ is smaller than $\lambda_{Ki},\ \in \mathcal{V}$ from the definition in (40). Therefore, when (40) is satisfied,

$$\dot{S} \leq -\underline{\kappa}\|e\|^2 + \frac{n\gamma^2}{2}\bar{\Delta}^2, \tag{49}$$

holds with probability δ. Analogous to [16, Theorem 1], the error e is proven to be uniformly ultimately bounded from (49) and [21]. The ultimate bound of (42) is also derived in the same way. ■

Theorem 3 implies that (20) is satisfied with B of (42) with probability. Since (42) is almost the same form as the ultimate bound in [16], this result can be regarded as a natural extension. To reduce the ultimate bound in [16], we need to set the gain K_i larger. In this paper, by properly designing the structure of the graph $\mathcal{G}$ and k_s, we can reduce the ultimate bound and expect to improve the pursuit performance.

V. SIMULATIONS

In this simulation, we consider a target with position dependent motion and compare the results with (24) and (30). We also compare the performance difference between the graphs $\mathcal{G}$ and k_s. Because we focus on the effect of communication, K_i are designed to be constant.

We consider 3 robots, and the visibility set is specified by $\mathcal{V}_v = \{1, 2\}$. Two graphs are considered, $\mathcal{G}_1$ and $\mathcal{G}_2$, shown in Fig. 4. The desired poses g_{di} are designed so that the target is inside the triangle formed by robots as in Fig. 4.

The translational velocity is given as

$$v_{w0}^b = 0.3 \begin{bmatrix} [p_{w0}]_2 \\ -[p_{w0}]_1 + (1 - [p_{w0}]_1^2)[p_{w0}]_2 \\ ([p_{w0}]_1)/r_p \end{bmatrix}, \tag{50}$$

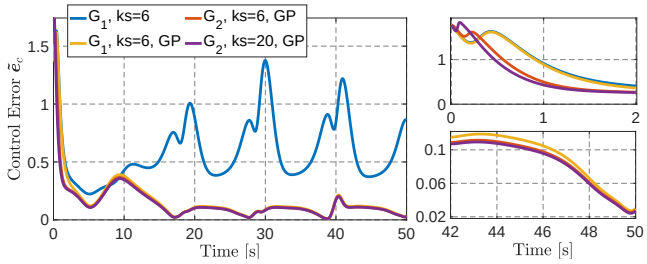

Fig. 6: Comparison of control error norms $\|\tilde{e}_c\|$.

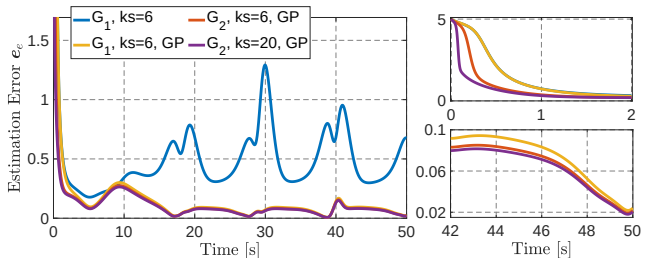

Fig. 7: Comparison of estimation error norms $\|e_e\|$.

where $r_p \coloneqq \sqrt{[p_{w0}]_1^2 + [p_{w0}]_2^2}$, and the angular velocity is

$$\omega_{w0}^b = 0.3[\ 0\ 0\ (\pi[p_{w0}]_1)/(8r_p)\ ]^\top. \tag{51}$$

The trajectory of the target position is shown in Fig. 5. In xy-plane, the trajectory is generated by a Van der Pol oscillator. The training data $\mathcal{D}$ is shown as the red crosses in Fig. 5 and is shared by all robots. The hyperparameters are trained by evidence maximum with 15 data points. Then, the Lipschitz constant L_μ is calculated as 1.2. The gains are $K_{ci} = 8I_6$, $K_{ei} = 8I_6$ for all $i \in \{1, 2, 3\}$ and $\gamma = \sqrt{10}$. In this case, $\underline{\kappa} = 0.091$ with $k_s = 6$, which satisfy the condition (40).

Fig. 6 shows the control error $\tilde{e}_c = [\tilde{e}_{c1}^\top\ \tilde{e}_{c2}^\top\ \tilde{e}_{c3}^\top]^\top$ in (11) instead of (15) to see the difference between the desired and real poses. The blue and yellow lines show the results with the control law (24) and (30), respectively. From the figures, it is observed that the performance of control and estimation is significantly improved by integration a GP model.

For further analyses with the control law (30), the graph $\mathcal{G}_1$ is changed to $\mathcal{G}_2$ (red line, $\underline{\kappa} = 0.77$) and in addition, k_s is updated to 20 (purple line, $\underline{\kappa} = 1.2$). The upper right graphs in Figs. 6 and 7 show that the errors decrease faster with larger $\underline{\kappa}$. The lower right graphs in Figs. 6 and 7 also show that the cases with larger $\underline{\kappa}$ have smaller errors. This is also confirmed from the ultimate bound (42) because larger $\underline{\kappa}$ is required to reduce B. From the fact that adding the edge between robot 2 and 3, and larger k_s resulted in larger $\underline{\kappa}$, it is concluded that the robots in $\bar{\mathcal{V}}_v$ need strong interconnections with the robots in $\mathcal{V}_v$ for better pursuit performance.

VI. CONCLUSIONS

In this paper, we proposed a cooperative visual pursuit control law based on motion estimation and a target velocity model by a Gaussian process. First, we derived a cooperative visual pursuit control law from passivity of rigid body motion and extended it by integrating a trained GP model. Second, we proved that if the target is static, the proposed control law achieves cooperative visual pursuit if at least one robot can obtain visual information of the target. Furthermore, we also showed that the estimation and control errors are ultimately bounded with high probability by the proposed control law for the moving target. Finally, we demonstrated the effectiveness of the proposed scheme through simulations.

REFERENCES

[1] S. A. P. Quintero, D. A. Copp, and J. P. Hespanha, "Robust Coordination of Small UAVs for Vision-based Target Tracking Using Output-Feedback MPC with MHE," in *Cooperative Control of Multi-Agent Systems*, Y. Wang *et al.*, Eds. Wiley, 2017, pp. 51–83.

[2] T. Hatanaka, N. Chopra, M. Fujita, and M. W. Spong, *Passivity-Based Control and Estimation in Networked Robotics*. Springer, 2015.

[3] N. Wahlström, T. B. Schön, and M. P. Deisenroth, "From Pixels to Torques: Policy Learning with Deep Dynamical Models," *Deep Learning Workshop at the 32nd International Conference on Machine Learning*, 2015.

[4] K. Shah, G. Ballard, A. Schmidt, and M. Schwager, "Multidrone Aerial Surveys of Penguin Colonies in Antarctica," *Science Robotics*, vol. 5, no. 47, eabc3000, 2020.

[5] A. A. Paranjape, S.-J. Chung, K. Kim, and D. H. Shim, "Robotic Herding of a Flock of Birds Using an Unmanned Aerial Vehicle," *IEEE Trans. Robot.*, vol. 34, no. 4, pp. 901–915, 2017.

[6] M. W. Spong, S. Hutchinson, and M. Vidyasagar, *Robot Modeling and Control*, 2nd ed. Wiley, 2020.

[7] L. D. Fairfax and P. A. Vela, "A Concurrent Learning Approach to Monocular, Vision-Based Regulation of Leader/Follower Systems," *Proc. American Control Conference*, pp. 3502–3507, 2018.

[8] A. Khosravian, J. Trumpf, R. Mahony, and C. Lageman, "Observers for Invariant Systems on Lie Groups with Biased Input Measurements and Homogeneous Outputs," *Automatica*, vol. 55, pp. 19–26, 2015.

[9] D. Chwa, A. P. Dani, and W. E. Dixon, "Range and Motion Estimation of a Monocular Camera Using Static and Moving Objects," *IEEE Trans. Control Syst. Technol.*, vol. 24, no. 4, pp. 1174–1183, 2016.

[10] T. Hatanaka and M. Fujita, "Cooperative Estimation of Averaged 3-D Moving Target Poses via Networked Visual Motion Observer," *IEEE Trans. Autom. Control*, vol. 58, no. 3, pp. 623–638, 2013.

[11] C. E. Rasmussen and C. K. I. Williams, *Gaussian Processes for Machine Learning*. MIT Press, 2006.

[12] G. Chowdhary, H. A. Kingravi, J. P. How, and P. A. Vela, "Bayesian Nonparametric Adaptive Control Using Gaussian Processes," *IEEE Trans. Neural Netw. Learn. Syst.*, vol. 26, no. 3, pp. 537–550, 2015.

[13] F. Berkenkamp, R. Moriconi, A. P. Schoellig, and A. Krause, "Safe Learning of Regions of Attraction for Uncertain, Nonlinear Systems with Gaussian Processes," *Proc. 55th IEEE Conference on Decision and Control*, pp. 4661–4666, 2016.

[14] T. Beckers, D. Kulić, and S. Hirche, "Stable Gaussian Process Based Tracking Control of Euler–Lagrange Systems," *Automatica*, vol. 103, pp. 390–397, 2019.

[15] Y. Ito, K. Fujimoto, and Y. Tadokoro, "Kernel-Based Hamilton–Jacobi Equations for Data-Driven Optimal and H-Infinity Control," *IEEE Access*, vol. 8, pp. 131 047–131 062, 2020.

[16] J. Yamauchi, T. Beckers, M. Omainska, T. Hatanaka, S. Hirche, and M. Fujita, "Visual Pursuit Control with Target Motion Learning via Gaussian Process," *Proc. 59th SICE Annual Conference*, pp. 1365–1372, 2020.

[17] M. Mesbahi and M. Egerstedt, *Graph Theoretic Methods in Multiagent Networks*. Princeton University Press, 2010.

[18] G. A. Kane, G. Lopes, J. L. Saunders, A. Mathis, and M. W. Mathis, "Real-Time, Low-Latency Closed-Loop Feedback using Markerless Posture Tracking," *eLife*, vol. 9, e61909, 2020.

[19] T. Hatanaka, Y. Igarashi, M. Fujita, and M. W. Spong, "Passivity-Based Pose Synchronization in Three Dimensions," *IEEE Trans. Autom. Control*, vol. 57, no. 2, pp. 360 – 375, 2012.

[20] N. Srinivas, A. Krause, S. M. Kakade, and M. W. Seeger, "Information-Theoretic Regret Bounds for Gaussian Process Optimization in the Bandit Setting," *IEEE Trans. Inf. Theory*, vol. 58, no. 5, pp. 3250–3265, 2012.

[21] H. Khalil, *Nonlinear Systems*, 3rd ed. Prentice Hall, 2002.